Transduction of Non-Small Cell Lung Cancer Cells by Adenoviral and Retroviral Vectors

Raj K. Batra, John C. Olsen, Raymond J. Pickles, Diana K. Hoganson, and Richard C. Boucher

Cystic Fibrosis/Pulmonary Research and Treatment Center, School of Medicine, The University of North Carolina at Chapel Hill, Chapel Hill, North Carolina

Gene transfer into a panel of non-small cell lung cancer (NSCLC) cells by adenoviral (Ad) and retroviral (RV) vectors was studied. Indexed to multiplicity of infection (MOI), Ad vectors transduce squamous, adenosquamous, and malignant mesothelioma cells with greater efficiency than large cells or adenocarcinoma cells. Transduction-sensitive cells bind the Ad vector with specificity for the Ad fiber knob, and internalize vector efficiently. Transduction-refractory cells bind and internalize vector by less efficient pathways. Like Ad vectors, there is heterogeneity in RV transduction efficiencies of different NSCLC subtypes. With respect to the most common cell type metastatic to the pleural space (adenocarcinoma), amphotropic retroviral vectors transduce cells of this subtype more efficiently (at a lower MOI) than Ad. RV transduction is not solely dependent on cellular replication, and both permissive and refractory cell lines express the mRNA for the amphotropic RV receptor. These observations suggest that neither Ad nor RV vectors will suffice *a priori* as the optimal gene transfer vehicle, and successful gene therapy of lung cancer may require tumor-specific or patient-specific vectors. **Batra, R. K., J. C. Olsen, R. J. Pickles, D. K. Hoganson, and R. C. Boucher. 1998. Transduction of non-small cell lung cancer cells by adenoviral and retroviral vectors. Am. J. Respir. Cell Mol. Biol. 18:402–410.**

Lung cancer is the leading cause of cancer mortality in the United States. Despite gains in survival and quality of life using conventional multimodality (chemotherapy, radiation, and surgery) approaches, this disease results in 160,000 deaths annually. As a result, newer biologic therapeutic strategies, including gene therapy, are being developed. Among these, tumor-suppressor gene replacement ther-

apy (1), immunomodulatory and genetic vaccination strategies (2–4), drug-sensitizing or "suicide gene" therapy (5, 6), and antisense therapy targeting oncogene products (7, 8) are examples of proposed conceptual approaches. Irrespective of the paradigm, it is likely that efficient gene transfer into target cells *in vivo* will be required for the successful gene therapy of lung cancer. The target cells in many of the approaches are tumor cells, and given the various cellular subtypes that comprise lung cancer, it is unclear whether a single vector will suffice for gene delivery.

To date, gene transfer is most efficient using viral vectors, and two such vectors are commonly associated with humans. The adenoviral vector is a transient expression system that can be generated at high titer (9), and on the basis of previous reports is promiscuous for targeting a variety of cell types (10). The general steps mediating adenoviral transduction are: (*1*) binding with high affinity to a specific cell surface receptor (11, 12); (*2*) receptor-mediated endocytosis into the target cell mediated in part by specific cell surface integrins (13, 14); (*3*) endosomal escape and intracellular transport to the nuclear pore (15, 16); and (*4*) episomal expression of the vector DNA. The retroviral (RV) vector is integrative and can be generated only in lower titers. The general steps mediating amphotropic retroviral transduction are characterized as: (*1*) binding of a viral envelope glycoprotein specifically to a target cell receptor (17, 18); (*2*) fusion of the virus with the target cell plasma membrane; (*3*) reverse transcription and

transport of the vector DNA to the nucleus during disassembly in mitosis; and (*4*) proviral integration and transgene expression (19). Because the latter steps for RV transduction require cellular turnover (20), the Moloney murine leukemia virus (Mo-MuLV)-based RV system may potentially enable targeting specificity for cancer cells (i.e., replicating cells) in selected systems (e.g., brain tumors).

We have chosen malignant pleural effusions as a "proof-of-concept" clinical model, and hypothesize that principles of vector targeting in this model may have implications for the treatment of lung cancer in general. These preclinical studies were designed to identify the most efficient vector for targeting various non-small cell lung cancer (NSCLC) cells in the pleural space, and focused on comparing adenoviral (Ad) and RV vectors in *in vitro* studies. Therefore, the cell lines used for these studies were primarily derived from the pleural space to model the relevant target cell population. To compare the relative efficiency of gene transfer vectors, we indexed transduction (as measured by reporter gene expression) to multiplicity of infection (MOI, number of infectious particles per target cell). In addition, although all histopathologic subtypes can lead to malignant pleural effusions, they result most commonly from lung adenocarcinoma metastatic to the pleural space (21). Therefore, particular attention was given to the vector-mediated transduction of this NSCLC subtype. Finally, because of the observed differences in vector-specific transduction of different NSCLC subtypes, an evaluation of the underlying mechanisms affecting transduction efficiency by both the adenoviral and retroviral vectors was performed.

Materials and Methods
Cell Lines

Cell lines were a gift of Dr. Herbert Oie at the National Cancer Institute (NCI), and were maintained in RPMI 1640 (GIBCO-BRL, Gaithersburg, MD) with 10% fetal bovine serum (GIBCO-BRL) and penicillin (100 U/ml)–streptomycin (100 μg/ml) (R_{10}; GIBCO-BRL). Many of these cell lines were described with respect to their morphologic and genetic profile by Dr. Adi Gazdar and colleagues (22–25), and detailed characteristics of all lines is provided in the NCI-Navy Medical Oncology Branch Cell Line Data Base (26). To target the appropriate cells *in vitro*, a panel of NSCLC subtypes derived from the pleural space and representing a broad spectrum of lung cancer and mesothelial malignancy (NCI-H28, NCI-H226, NCI-H460, NCI-H647, and NCI-H1437) was initially studied. Because the majority of intrapleural metastases arise from lung adenocarcinoma, a panel representing this specific NSCLC subtype (NCI-H441, NCI-H1650, NCI-H1666, and NCI-H2122) was investigated in greater detail. To assess the generalizability of the observed differential transduction, studies were also performed on a different set of squamous cell cancer cell lines (NCI-H157 and NCI-H1703). Mv1Lu cells, a lung epithelial cell line easily infectable with retroviruses, were obtained from the American Type Cell Culture (ATCC, Rockville, MD) and maintained in Eagle's minimal essential medium (MEM) containing 10% fetal bovine serum and penicillin–streptomycin (M_{10}).

Viral Vectors

Adenoviral vectors (Ad5CMVLacZ) were constructed in the Vector Core at the Gene Therapy Center of the University of North Carolina School of Medicine (Chapel Hill, NC). These adenovirus serotype 5 (Ad5) vectors were E1a/E1b and partially E3 deleted, and expressed the *Escherichia coli lacZ* gene as the reporter under the regulation of the cytomegalovirus (CMV) immediate-early promoter region (27). The adenoviral vector stocks ranged from 1.5×10^{12} to 3×10^{13} particles/ml as measured by optical density measured at 260 nm (OD_{260}), with titers (derived from plaque assays of 293 cells) of 1.7×10^{10} and 6.6×10^{11} plaque-forming units (pfu)/ml, respectively. ^{35}S-labeled Ad5 vectors, produced in the Vector Core at concentrations of $\sim 10^{12}$ particles/ml (specific activity, 2–3 $\times$ 10^{-3} counts per minute [cpm]/particle), were used to quantitate cellular binding and internalization (28). Adenoviral vectors were purified and concentrated with double CsCl ultracentrifugation and stored at $-20°$C in a nonfreezing solution containing 25% glycerol, 0.05% bovine serum albumin (BSA), 4 M CsCl, 50 mM NaCl, 0.5 mM $MgCl_2$, and 5 mM Tris-HCl (pH 8). Immediately before use, vectors were gel-filtered (G-50 Sephadex; Boehringer Mannheim, Indianapolis, IN) and eluted into R_{10} medium for transduction studies. Recovery of vector, as measured by absorbance at 260 nm ($A_{260\ nm}$) or radiocounts, is reliably 70–100% using this desalting procedure.

The amphotropic retroviral vector employed in this study, LNPOZ, was produced using the helper-free cell line PA.LNPOZ.1 as described (29, 30). LNPOZ vectors link the neomycin selection marker and the reporter *lacZ* gene by a poliovirus internal ribosomal entry site (IRES) sequence for the generation of a single transcript from the inserted provirus. Titers were measured by NIH 3T3 transduction assays counting G-418-resistant colonies and generally ranged from 0.5×10^6 to 2×10^6 cfu/ml.

Transduction Protocols

Twenty-four hours before transduction, $1–2 \times 10^5$ target cells were seeded into each well of 6-well (3.5-cm) plates (Costar, Cambridge, MA) with 2 ml of growth medium. On the day of transduction, the MOI for the vector was determined by dividing the vector plaque-forming units by the number of target cells detached (using 1% trypsin–1 mM EDTA) and counted (using a hemacytometer) from a representative well. Serial dilutions (1:10) of the vector were made in growth medium, and 1-ml aliquots were applied to each well.

Ad vectors at various MOIs were incubated with the target cells for 0.75 h at 37°C, 5% CO_2, following which the cells were washed with phosphate-buffered saline (PBS), growth medium was replaced, and the cells were maintained at 37°C, 5% CO_2 until expression analysis. In subsequent studies, the adenoviral vector was incubated with target cells at an MOI of 50 for various time intervals.

As a quality control for different preparations of amphotropic RV vectors, Mv1Lu cells were included in the experimental design because these cells exhibited a consistent and predictable infectivity by the RV vectors at MOIs of 0.1–10. The amphotropic retroviral vectors were incu-

bated with the target cells in the presence of 8 μg/ml Poly-brene for 2 h, the vector aspirated, the cells washed with PBS, growth medium replaced, and the cells maintained at 37°C, 5% CO_2 until expression analysis.

Transgene Expression Analysis

Transduction efficiency was assayed by *lacZ* gene expression at 24 or 48 h following adenoviral or retroviral transduction, respectively. Histochemical analysis was performed by assaying for intracellular 5-bromo-4-chloro-3-indoyl-β-D-galactopyranoside (X-Gal; 5 Prime-3 Prime, Boulder, CO) hydrolysis in fixed (0.5% glutaraldehyde for 10 min, 4°C) target cells (31, 32), and the percentage of positive cells determined. The expression of *lacZ* was also measured using flow cytometry (FAC-Scan; Becton Dickinson, Mountain View, CA) by surveying 16,000 cells for the intracellular hydrolysis of fluorescein di-β-D-galactopyranoside (FDG; Molecular Probes, Eugene, OR) (33). For these studies, the target cells were detached, resuspended in 100 μl of growth medium, exposed to 1 mM FDG in hypotonic medium (100 μl of water containing 1.0% dimethyl sulfoxide) for 1 min at 37°C, and the substrate loading stopped with the addition of cold medium containing 1 μg/ml propidium iodide (PI). Cells that incorporated PI (red fluorescence) were defined as nonviable and excluded from analysis at the time of data acquisition. The transduced cell population constituted those cells exhibiting green fluorescence exceeding the 99th percentile of a control population that was not transduced with vector but was exposed to hypotonic shock and FDG loading.

Cell Proliferation Analyses

To compare the relative proliferative rates of the various lung cancer cell lines, the cells were pulsed for 2 h with 5-bromo-2′-deoxyuridine (BrdU; Boehringer Mannheim). After a PBS wash, the cells were fixed in absolute methanol, and the cellular DNA was denatured in 2 N HCl for 2 h at 37°C. Following neutralization with 0.1 M sodium borate (pH 8.5), the cells were incubated with 50 μg/ml anti-bromodeoxyuridine fluoroscein conjugate for 1 h. At least 200 cells per slide were counted in random high-power fields using fluorescence microscopy, and the percentage of labeled (proliferating) cells determined in three separate experiments.

Adenoviral Binding Analyses

All binding studies were performed at 4°C using an ^{35}S-labeled adenoviral vector (^{35}S-Ad5 vector; specific activity, 1–3 $\times$ 10^{-3} cpm/particle) at a particle-to-cell ratio of 1,000 to 10,000:1. At various time intervals (0, 0.75, 3, 6, 10, and 30 h), unbound ^{35}S-Ad5 vector was collected in two PBS washes and radiocounted. Next, the cell-bound fraction was quantitated by cell lysis (1 ml of 0.3 N NaOH plus 1% sodium dodecyl sulfate [SDS]: lysis buffer) and ^{35}S radio-counting. Specific binding to target cells was studied by competing with 10 μg/ml Ad5 fiber knob (a kind gift from Dr. Joanne T. Douglas, Gene Therapy Program, University of Alabama, Birmingham), which was coincubated with the radiolabeled Ad during exposure to target cells (34).

Adenoviral Internalization Analyses

To determine the kinetics of adenoviral internalization, 5 $\times$ 10^5 target cells were exposed to the ^{35}S-Ad5 vector (particle-to-cell ratio, 10,000:1) at 37°C, 5% CO_2 at time intervals that paralleled the binding experiments. The unbound fraction in medium was removed by rinsing cells twice with PBS, followed by an acid–salt (0.2 M acetic acid in 0.5 M NaCl) wash and proteinase treatment (0.25% protease XIV at 4°C for 1 h). The internalized ^{35}S-Ad5 component was collected by solubilizing the cells in lysis buffer. The efficiency of internalization of bound vector was calculated by dividing the internalized counts by the bound counts from parallel plates at the 0.75-h time interval.

RAM-1 Northern Analysis

A 481-base pair (bp) fragment of the amphotropic retroviral receptor (RAM-1) mRNA (bp 794–1,275) was amplified following reverse transcription (RTth DNA polymerase; Perkin-Elmer, Branchburg, NJ) of CFT1 total cellular RNA (35) harvested using the Trisolv (Biotecx, Houston, TX) reagent. This fragment was inserted into the pCRII cloning vector, amplified (TA cloning system; Invitrogen, San Diego, CA), and the gel-purified insert was used to make a ^{32}P-labeled probe using the random primed DNA-labeling method (Boehringer Manneheim).

Twelve micrograms of total cellular RNA from various tumor cells in log-phase growth was electrophoresed in a 5% formaldehyde–1.2% agarose gel and transferred onto a nylon membrane (Stratagene, La Jolla, CA). Northern hybridization with total cellular RNA was performed using the RAM-1 probe (activity, 2.7 $\times$ 10^8 cpm/ml) overnight at a hybridization temperature of 68°C. Membranes were washed three times with 2$\times$ saline sodium citrate (SSC) plus 0.1% SDS at room temperature for 45 min and once with 0.1$\times$ SSC plus 1% SDS at 60°C for 90 min, exposed to film overnight at -70°C, and the autoradiogram developed 24 h later.

Statistical Methods

Data are reported as the mean $\pm$ the standard error of the mean, with the overall statistical significance of differences within the groups determined using Kruskal–Wallis analysis of variance (ANOVA) on ranks, followed by Bonferroni group comparisons (Figure 2). The statistical significance of the differences for Ad vector binding and internalization (Figures 3 and 4) was determined using the unpaired two-tailed *t* test. Transduction efficiencies of the adenoviral and retroviral vectors (Figures 1 and 5) were compared using probit analysis (36). Specifically, the curves of percent transduction versus MOI (logarithmic values) were fit for probit analysis using the Statistical Analysis System (SAS version 6.10; SAS, Cary, NC). This method provides 95% fiducial intervals (95% FI) for specified transduction percentages (25% transduction used for all comparisons). Nonoverlapping fiducial intervals for 25% transduction efficiency is taken as evidence of a statistically significant difference ($P < 0.05$) between the cell lines compared.

Results

Figure 1A depicts the range of adenoviral transduction efficiencies in a variety of histopathologic subtypes of lung cancer cell lines derived from intrapleural metastases. The adenoviral vector transduces squamous cell cancer (H226), adenosquamous (H647), and malignant mesothelioma (H28) cell lines one to three orders of magnitude lower MOIs than the adenocarcinoma (H1437) and large cell (H460) cancer lines. Given these unexpected results, we next tested whether this differential transduction was generalizable to other lung squamous cell cancer and adenocarcinoma cell lines. Three different squamous cell cancers (H157, H226, and H1703) are all transduced with the adenoviral vectors with similar efficiency (Figure 1B), and as shown in Figure 1C, a variety of lung adenocarcinomas (H441, H1437, H1650,

H1666, and H2122) are relatively refractory to adenoviral transduction when compared to the squamous cell cancers. Among the group of lung adenocarcinomas, the cell lines derived from bronchoalveolar cell cancers (H358 [not shown] and H441; peripheral airway cancers) are the most susceptible, and the H2122 cell line the least susceptible to adenoviral transduction. It is noteworthy, however, that all the adenocarcinoma cell lines can be transduced when exposed to the adenoviral vector at high (> 100) MOIs (Figure 1C).

We next evaluated the mechanisms that determine the differences in the adenoviral transduction efficiency of the squamous cell versus the adenocarcinoma cell lines. Because differences in adenoviral entry (binding and/or internalization) may be rate limiting for transduction, we compared these properties in the permissive squamous
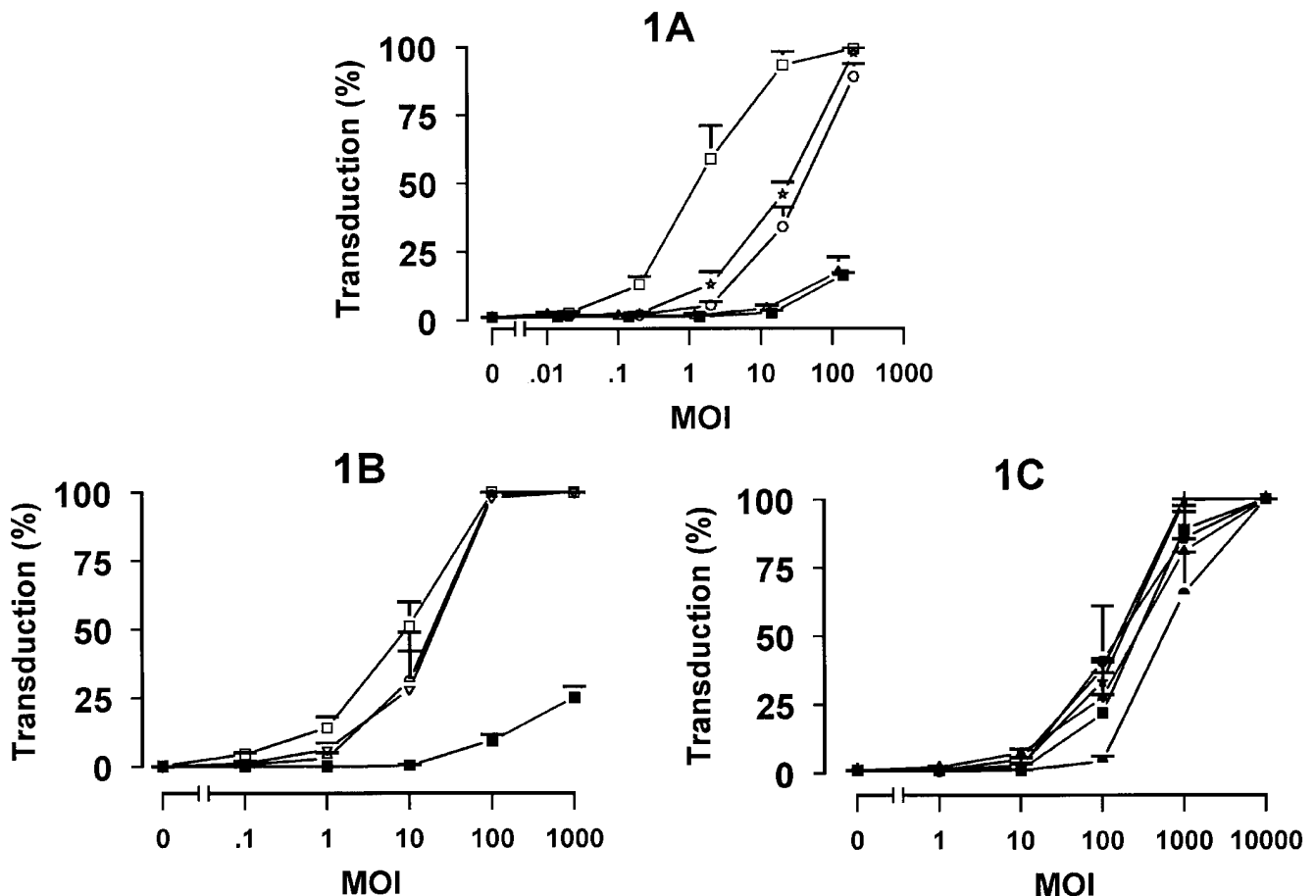
Figure 1. (*A*) Comparison of adenoviral transduction of NSCLC subtypes or malignant mesothelioma as a function of MOI. Target cells were exposed to a *lacZ* adenoviral vector at various MOIs for 45 min, and transduction efficiency (expression of β-galactosidase) measured 24 h later by flow cytometry. *Open circles*, H28 (malignant mesothelioma); *open squares*, H226 (squamous cell carcinoma); *open triangles*, H460 (large cell lung cancer); *open stars*, H647 (adenosquamous lung cancer); *solid squares*, H1437 (lung adenocarcinoma). Data are presented as mean ± SEM of four experiments. (*B*) Comparison of adenoviral transduction of NSCLC squamous cell lung cancer cells (*open symbols*) versus adenocarcinoma (H1437) cells (*solid symbols*) as a function of MOI. Target cells were exposed to a *lacZ* adenoviral vector at various MOIs for 45 min, and transduction efficiency measured 24 h later by histochemistry. *Open squares*, H226; *inverse open triangles*, H157 (squamous cell lung cancer); *open half-circles*, H1703 (squamous cell carcinomas); *solid squares*, H1437 (lung adenocarcinoma). Data are presented as mean ± SEM of three experiments. (*C*) Adenoviral transduction of various NSCLC-adenocarcinoma cells. Target cells were exposed to a *lacZ* adenoviral vector at various MOIs for 45 min, and transduction efficiency measured 24 h later by flow cytometry. *Solid circles*, H441 (lung adenocarcinoma); *solid squares*, H1437 (lung adenocarcinoma); *solid triangles*, H1650 (lung adenocarcinoma); *solid stars*, H1666 (lung adenocarcinoma); *solid half-circles*, H2122 (lung adenocarcinoma). Data are presented as mean ± SEM of four experiments.

cell (H226, 1703) versus relatively nonpermissive adeno-carcinoma (H1437, H2122) cell types. The results of the 1-h binding studies (performed at 4°C at an Ad cpm/cell ratio of 3) demonstrate that the squamous cell cancers bind more vector than do the adenocarcinoma cells (Figure 2). Moreover, excess fiber knob (10 μg/ml; greater than 1,000-fold excess of Ad particles/cell) inhibits Ad binding in the squamous cell cancers, but does not appear to impact Ad binding to the adenocarcinoma cells. These results suggest that binding to the permissive cells is occurring via a specific cell–Ad fiber knob interaction, and by a different, nonspecific binding mechanism in the transduction-refractory cell types. Thus, these results indicate that differences in adenoviral binding may contribute to differences in the transduction efficiencies of individual cell lines.

In a separate series of experiments, the kinetics of Ad entry into a squamous cell cancer (H226) and an adeno-carcinoma (H1437) cell line were compared. As shown in Figure 3A, the squamous cell cancer line H226 binds (at 4°C) significantly more vector at all time points than the adenocarcinoma cell line (H1437). Both cell types bind more vector over time, and the absolute quantity of adenovirus bound by the squamous cell cancer at 0.75 h is roughly equivalent to that bound by the adenocarcinoma at 10 h. The efficiently transduced squamous cell cancer line also internalizes more vector at all time points than the adenocarcinoma cell line (Figure 3B). The kinetics of viral entry into the permissive cells can be described by a fast linear component that appears to saturate following the 10-h time point. In contrast, the internalization of ^{35}S-Ad vector into the adenocarcinoma cell line is linear and significantly slower at each time point compared to the squamous cell cancer. The efficiency of internalization of

bound vector (i.e., percentage internalized divided by bound plus cell surface-associated ^{35}S-Ad vector) was determined 0.75 h following adenoviral exposure (in an effort to minimize the role of receptor recycling), and is very high (100%) for the squamous cell cancer line in contrast to the adenocarcinoma cell line (< 20%). These data indicate that Ad internalization is more efficient for the H226 than the H1437 cell line, and also contributes to relative disparity of gene transfer efficiency into these subtypes.

It is notable that internalization of Ad into all target cells increases with prolonged exposure to the virus (Figure 3B). The data show that the quantity of Ad internalized by the transduction-refractory H1437 cell line at 30 h approximates that internalized by the transduction-sensitive H226 cell line by 3 h, suggesting that the relative inefficiency of transduction of the lung adenocarcinoma cell lines may be overcome by prolonging the exposure of the vector to the target cells. To test this hypothesis, adenoviral vectors were exposed to the squamous cell (H226) and adenocarcinoma (H1437 and H2122) cell lines at an MOI of 50 for various time intervals ranging from 0.75 to 24 h. As predicted, whereas the squamous cell cancer is rapidly and efficiently transduced, prolonging the duration of exposure to the adenoviral vector permits transduction of the adenocarcinoma cell lines (Figure 4). Indeed, a 24-h exposure of the vector to the most transduction-resistant lung adenocarcinoma studied (H2122) results in nearly uniform cellular transduction.

Transduction efficiencies of NSCLC cell lines were also investigated using the amphotropic retroviral vector. The range of MOIs tested is limited for the amphotropic RV vector because of the difficulty in concentrating this vector
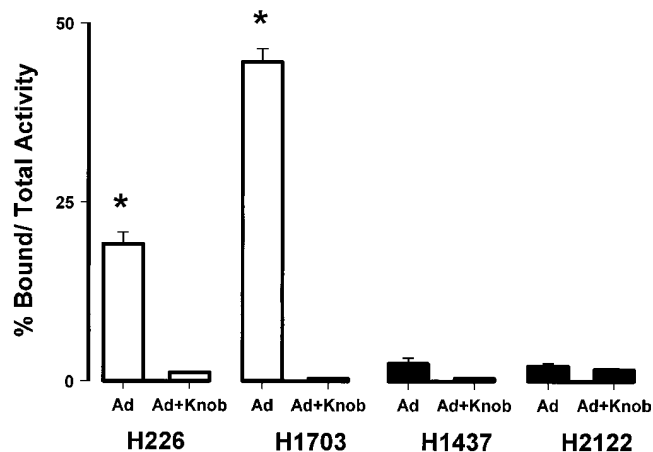
Figure 2. Comparison of adenoviral binding to transduction-sensitive squamous cell cancer cells (H226, H1703; open bars) versus transduction-resistant adenocarcinoma cells (H1437, H2122; shaded bars). Radiolabeled Ad is exposed to target cells at 4°C in the absence or presence of 10 μg/ml adenoviral fiber knob for 1 h, and cell-bound vector counted. Data are presented as mean ± SEM of ^{35}S radiocounts from three separate samples at each time point. *P < 0.001 by ANOVA on ranks followed by Bonferroni group comparisons for a statistically significant difference between groups.
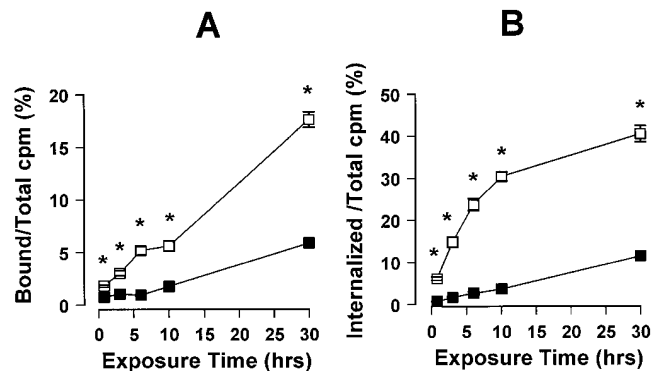
Figure 3. (A) Comparison of adenoviral binding to a squamous cell line (open squares, H226) versus a lung adenocarcinoma cell line (solid squares, H1437) as a function of time. At 4°C, target cells were exposed to radiolabeled adenoviral vector, and the percentage bound vector quantified over time. Data are presented as mean ± SEM of ^{35}S radiocounts from six samples at each time point. (B) Comparison of adenoviral internalization into a squamous cell line (open squares, H226) versus an adenocarcinoma cell line (solid squares, H1437) as a function of time. At 37°C, target cells were exposed to radiolabeled adenoviral vector, and the percentage internalized vector quantified over time. Data are presented as mean ± SEM of radiocounts from four samples at each time point. *P < 0.001 by the unpaired two-tailed t test for a statistically significant difference between the two groups at various times.
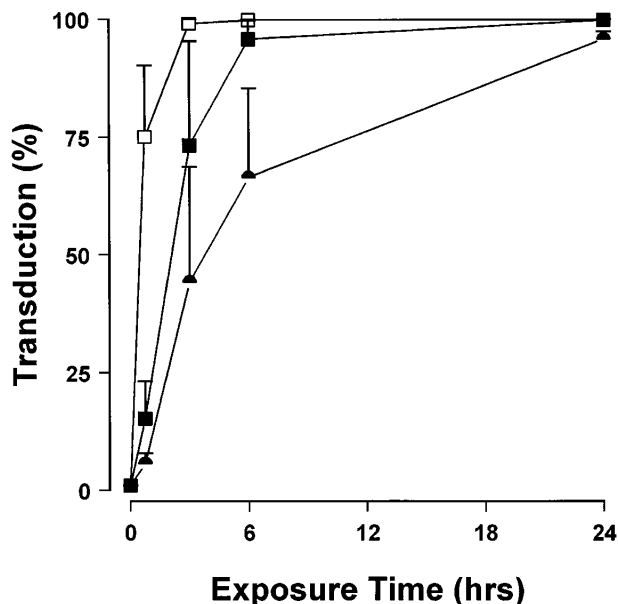
Figure 4. Comparison of the kinetics of Ad transduction of a squamous cell line (*open squares*, H226) versus lung adenocarcinoma cell lines (*solid squares*, H1437; *solid half-circles*, H2122) as a function of time. Equal numbers of target cells were exposed to the *lacZ* adenoviral vector at an MOI of 50 for 0.75, 3, 6, 12, or 24 h, and transduction efficiency (expression of β-galactosidase) measured 24 h later by flow cytometry. Data are presented as mean ± SEM of three separate experiments. By probit analysis, a statistically significant ($P < 0.05$) difference exists between the curves with H226 > H1437 > H2122 in terms of expediency of Ad transduction.

to titers comparable with the Ad vectors. In contrast to the data for Ad vectors, adenocarcinoma (H1437) is transduced with significantly greater efficiency by the retroviral vector than the squamous cell cancer (H226) and mesothelioma (H28) cell lines (Figure 5A). The RV vectors reliably transduced 25–50% of the H1437 adenocarcinoma cells at MOIs of 1–5, whereas an adenoviral MOI of 100–1,000 is required to transduce the H1437 cells with comparable efficiency (Figures 1A and 1C). To determine whether the H1437 cell line is representative of other NSCLC adenocarcinomas, a panel of adenocarcinoma cell lines (H441, H1437, H1650, H1666, and H2122) was exposed to the amphotropic RV LNPOZ. A range of transduction efficiencies was noted for this NSCLC subtype (Figure 5B). For example, of the adenocarcinoma cell lines studied, the H1437 and H2122 cell lines are transduced with significantly greater efficiency than the H1650 and H1666 cell lines, and H441 (alveolar cell cancer) is relatively resistant to retroviral transduction. Therefore, it is unclear whether RV transduces in a "subtype-specific" pattern.

We investigated two variables that may contribute to RV transduction efficiency. First, because Mo-MuLV-based retroviral vectors transduce only dividing cells, we determined the proliferation status of the tumor cell lines. The results (Table 1) indicate that the proliferative fractions (as defined by BrdU positivity) among the target tumor cell populations are similar, suggesting that variability

in RV transduction cannot be ascribed simply to differences in proliferation rates. Second, we postulated that differences in transduction efficiency might reflect differences in RV binding/entry into the target cells. To study one component of RV entry, we measured amphotropic retroviral receptor (RAM-1) expression by Northern analysis in permissive (H1437 and H2122) and relatively nonpermissive (H226 and H441) cell lines. Both the permissive and relatively nonpermissive cell lines express detectable RAM-1 mRNA levels (Figure 6), suggesting that the disparate RV transduction efficiencies in these NSCLC cell lines are due to properties other than the steady state expression of receptor mRNA.

Discussion

Efficient *in vivo* gene transfer is a prerequisite for successful gene therapy for lung cancer. Currently, the most efficient gene transfer vehicles appear to be viral vectors. In this study, we sought to identify which viral vector would be optimal for targeting lung cancer by testing adenoviral and retroviral vectors in a spectrum of NSCLC subtypes. Adenoviral vectors most efficiently transduce squamous cell cancer lines, whereas adenocarcinoma and large cell cancer cell lines are relatively resistant to adenoviral transduction (Figures 1A through 1C). Although some variability exists in the transduction efficiencies between different cell lines of the same subtype, the NSCLC adenocarcinoma cell lines are generally more resistant to adenoviral transduction than squamous cell cancer lines (Figures 1B and 1C). However, the relative resistance to Ad transduction of the adenocarcinoma cell lines can be overcome by using high titers of the adenoviral vectors (Figure 1C).

Next, we studied the mechanisms that explain the range of transduction efficiencies observed using radiolabeled vectors to study adenoviral–target cell interactions. In the Ad-resistant adenocarcinoma cell lines H1437 and H2122, reductions in both the specific binding (Figures 2 and 3A) and internalization (Figure 3B) of the adenoviral vector are observed as compared with the transduction-sensitive squamous cell cancer lines H226 and H1703. The efficiency of entry of bound vectors was calculated and found to be greater for the H226 squamous cell line (100%) than for the H1437 adenocarcinoma cell line ($< 20\%$). Taken together, these findings suggest that the resistance to Ad gene transfer reflects reduced numbers of receptors and/or less efficient mechanisms mediating Ad binding and internalization.

Figures 3A and 3B demonstrate that Ad binding and internalization into NSCLC adenocarcinoma cells increases over time, suggesting that transduction efficiency can be enhanced by prolonging the duration of exposure to the vector. Indeed, in addition to increasing the MOI (Figure 1C), Ad transduction is increased at lower MOIs by prolonging incubation of the vector with the target cell (Figure 5). This observation may have relevance to our approach of targeting tumor in malignant pleural effusions, because the pathogenesis of these effusions is rooted in the lack of lymphatic clearance of the pleural space. Hence, in this setting, clearance of vector delivered into the pleural space will likely be limited, enabling prolonged interaction

Figure 5. (*A*) Comparison of amphotropic retroviral transduction of NSCLC subtypes, malignant mesothelioma, or Mv1Lu cells as a function of MOI. Target cells were exposed to a *lacZ* amphotropic retroviral vector at various MOIs for 2 h, and transduction efficiency (expression of β-galactosidase) measured 48 h later by flow cytometry. *Open diamonds*, Mv1Lu cells (a mink lung epithelial cell line that is highly transducible with these vectors); *open circles*, H28 (malignant mesothelioma); *open squares*, H226 (squamous cell carcinoma); *open triangles*, H460 (large cell lung cancer); *open stars*, H647 (adenosquamous lung cancer); *solid squares*, H1437 (lung adenocarcinoma). (*B*) Comparison of amphotropic RV transduction of various NSCLC adenocarcinomas as a function of MOI. Target cells were exposed to a *lacZ* amphotropic retroviral vector at various MOIs for 2 h, and transduction efficiency measured 48 h later by expression of β-galactosidase using flow cytometry. *Solid circles*, H441 (lung adenocarcinoma); *solid squares*, H1437 (lung adenocarcinoma); *solid triangles*, H1650 (lung adenocarcinoma); *solid stars*, H1666 (lung adenocarcinoma); *solid half-circles*, H2122 (lung adenocarcinoma). Data are presented as mean ± SEM of four experiments.
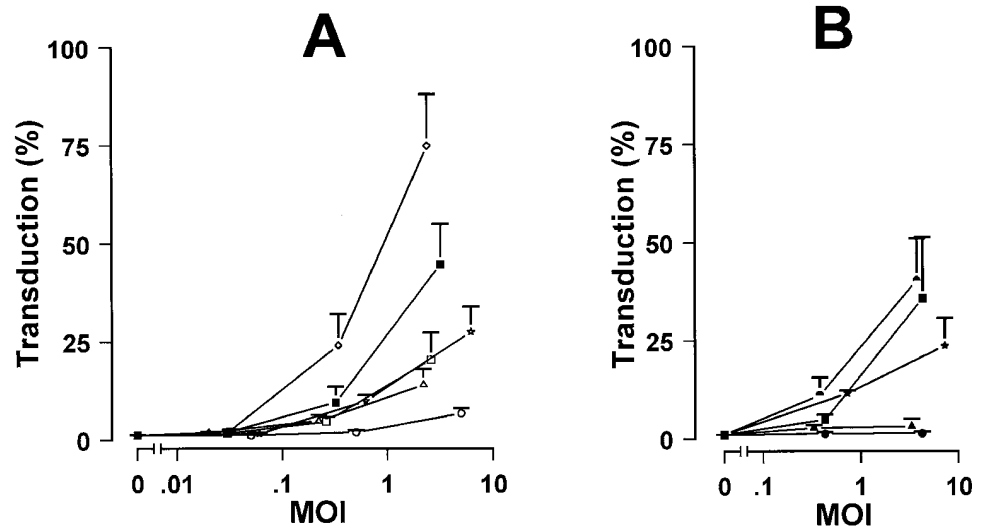
with the target cells and consequently optimizing the chances for transduction. Preliminary studies using an *in vivo* intracavitary model of lung adenocarcinoma suggest that H1437 cells can be readily transduced at low MOIs (1 to 10) *in vivo*, probably because in this model the vector is not cleared from the vicinity of the target cell.

Similar to the adenoviral vector, the retroviral vector transduces NSCLC subtypes *in vitro* (Figure 5A) with a wide range of transduction efficiencies. In fact, substantial variability is observed within a single histopathologic subtype (Figure 5B). Indexed to MOI, the data in general suggest that the amphotropic retroviral vector may be more efficient at transducing NSCLC adenocarcinoma cells than the adenoviral vector (Figure 5 versus Figure 1). Unfortunately, the inability to generate high-titer amphotropic retroviral vector makes it impossible to compare directly RV transduction over the ranges of MOI studied for the adenoviral vector.

We have studied two of the steps in the RV transduction scheme to identify the rate-limiting parameters that contribute to the diversity of transduction efficiencies exhibited by these vectors. First, the transduction efficiency is not a function of the proliferative rates of the target cells and all cell lines exhibited approximately equal replicating fractions (Table 1). Second, to explore the hypothesis that the variability reflects differences in retroviral entry, we measured the steady state expression levels of the mRNA for the amphotropic retroviral cell surface receptor (RAM-1) in permissive and relatively nonpermissive cell types. We found that both permissive and nonpermissive NSCLC cell types express RAM-1 by Northern analysis (Figure 6), suggesting that although expression of the receptor is probably required, it is not sufficient to mediate efficient transduction. Assuming that the steady state RAM-1 mRNA levels reflect functional cellular RV binding receptor numbers, these results suggest that the differences in the RV transduction efficiencies may be attributable to cellular processing of the vector after binding/entry. These data are congruent with those generated by others at this center regarding RV entry into well-differentiated versus poorly differentiated airway epithelial cell cultures, and suggest that reduced RV transduction of well-differentiated airway epithelia is not secondary to cellular turnover, but rather is a function of reduced RV adherence and internalization, and/or reduced reverse transcription of the vector following entry (37).

In conclusion, these *in vivo* studies were undertaken to characterize the efficiencies of vector targeting of lung cancer cells metastatic to the pleural space. With both viral vectors studied, we observed substantial variability in the

TABLE 1
Non-small cell or mesothelial derivation of the various cell lines used in this study

Cell Line	Derivation	% BrdU+*
H28	Malignant mesothelioma	46 ± 6
H157	Squamous cell lung cancer	
H226	Squamous cell lung cancer	45 ± 4
H441	Lung adenocarcinoma	
H460	Large cell lung cancer	53 ± 4
H647	Adenosquamous lung cancer	40 ± 9
H1437	Lung adenocarcinoma	49 ± 3
H1650	Lung adenocarcinoma	
H1666	Lung adenocarcinoma	
H1703	Squamous cell lung cancer	
H2122	Lung adenocarcinoma	
Mv1Lu	Mink lung epithelium	53 ± 4

* The fraction of cells proliferating (% BrdU+) over the time course of retroviral transduction is presented as the mean ± SEM of three separate measurements for several subtypes.
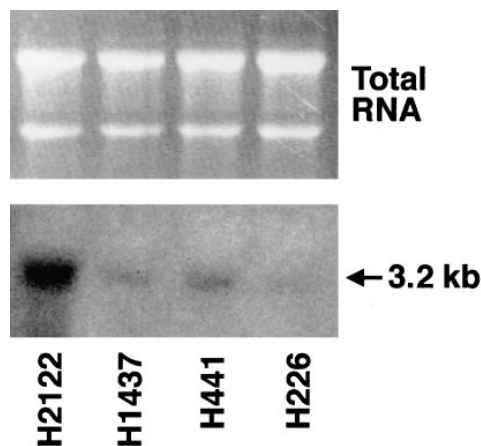
Figure 6. Comparison of the expression of RAM-1 (cellular amphotropic retroviral receptor) mRNA in cell lines permissive (H1437 and H2122) versus relatively nonpermissive (H226 and H441) for amphotropic retroviral transduction (Figures 5A and 5B) by Northern hybridization. (*Top*) Total cellular RNA loaded onto the gels. (*Bottom*) The 3.2-kb message as revealed by an overnight autoradiogram.

transduction efficiencies of cancer cells derived from different and even the same histopathologic subtypes of lung cancer. With respect to the adenoviral vector, the differences in transduction are in part due to the binding and rate of entry into the target cells, and resistance to adenoviral transduction may be overcome by increasing the MOI or by prolonging the duration of the vector to the target cells. With respect to the retroviral vectors, although they may be more efficient vehicles for transducing NSCLC adenocarcinomas than the adenoviral vectors *in vitro*, we have not been able to identify specific processes that predict gene transfer efficacy.

Given the limited numbers of cell lines tested, these results do not enable us to generalize our observations universally to all cultured NSCLCs, and because the expression and distribution of receptors mediating vector entry in tumor are largely unknown, we cannot make predictions regarding the *in vivo* transduction of NSCLC. There is a paucity of data correlating the behavior of vector–target cell interactions, and therefore gene transfer efficiency, *in vitro* as compared with *in vivo*, and more importantly, *in situ*. Consequently, it is clear that additional studies using the Ad and RV vectors in *in vivo* model systems that aptly mimic the human disease are needed before the optimal vector(s) for gene therapy of NSCLC can be resolved.

References

1. Roth, J. A., D. Nguyen, D. D. Lawrence, B. L. Kemp, C. H. Carrasco, D. Z. Ferson, W. K. Hong, R. Romaki, J. J. Lee, J. C. Nesbitt, K. M. W. Pisters, J. B. Putnam, R. Schea, D. M. Shin, G. L. Walsh, M. M. Dolormente, C. Han, F. D. Martin, N. Yen, K. Xu, L. C. Stephens, T. J. McDonnell, T. Mukhopadhyay, and D. Cai. 1996. Retrovirus-mediated wild-type p53 gene transfer to tumors of patients with lung cancer. *Nature Med.* 2:985–991.
2. Lee, C. T., H. L. Chen, and D. P. Carbone. 1995. Gene therapy for lung cancer. *Ann. Oncol.* 6(Suppl. 3):S61–S63.
3. Sharma, S., J. Wang, M. Huang, R. W. Paul, P. Lee, W. H. McBride, J. S. Economou, M. D. Roth, S. M. Kiertscher, and S. M. Dubinett. 1996. Interleukin-7 gene transfer in non-small-cell lung cancer decreases tumor proliferation, modifies cell surface molecular expression, and enhances antitumor reactivity. *Cancer Gene Ther.* 3:302–313.
4. Conry, R. M., G. Widera, A. F. LoBuglio, J. T. Fuller, S. E. Moore, D. L. Barlow, J. Turner, N. S. Yang, and D. T. Curiel. 1996. Selected strategies to augment polynucleotide immunization. *Gene Ther.* 3:67–74.
5. Hasegawa, Y., N. Emi, K. Shimokata, A. Abe, T. Kawabe, T. Hasegawa, T. Kirioka, and H. Saito. 1993. Gene transfer of herpes simplex virus type I thymidine kinase gene as a drug sensitivity gene into human lung cancer cell lines using retroviral vectors. *Am. J. Respir. Cell Mol. Biol.* 8:655–661.
6. Hwang, H. C., W. R. Smythe, A. A. Elshami, J. C. Kucharchzuk, K. M. Amin, J. P. Williams, L. A. Litzky, L. R. Kaiser, and S. M. Albelda. 1995. Gene therapy using adenovirus carrying the herpes simplex-thymidine kinase gene to treat *in vivo* models of human malignant mesothelioma and lung cancer. *Am. J. Respir. Cell Mol. Biol.* 13:7–16.
7. Zhang, W. W., and J. A. Roth. 1994. Anti-oncogene and tumor suppressor gene therapy—examples from a lung cancer animal model. *In Vivo* 8:755–769.
8. Roth, J. A. 1994. Modulation of oncogene and tumor-suppressor gene expression: a novel strategy for cancer prevention and treatment. *Ann. Surg. Oncol.* 1:79–86.
9. Curiel, D. T., J. M. Pilewski, and S. M. Albelda. 1996. Gene therapy approaches for inherited and acquired lung diseases. *Am. J. Respir. Cell Mol. Biol.* 14:1–18.
10. Mastrangeli, A., C. Danel, M. A. Rosenfeld, L. Stratford-Perricaudet, M. Perricaudet, A. Pavirani, J. Lecocq, and R. G. Crystal. 1993. Diversity of airway epithelial cell targets for *in vivo* recombinant adenovirus-mediated gene transfer. *J. Clin. Invest.* 91:225–234.
11. Bergelson, J. M., J. A. Cunningham, G. Droguett, E. A. Kurt-Jones, A. Krithivas, J. S. Hong, M. S. Horwitz, R. L. Crowell, and R. W. Finberg. 1997. Isolation of a common receptor for coxsackie B viruses and adenoviruses 2 and 5. *Science* 275:1320–1323.
12. Hong, S. S., L. Karayan, J. Tournier, D. T. Curiel, and P. A. Boulanger. 1997. Adenovirus type 5 fiber knob binds to MHC class I alpha2 domain at the surface of human epithelial and B lymphoblastoid cells. *EMBO J.* 16:2294–2306.
13. Wickham, T. J., P. Mathias, D. A. Cheresh, and G. R. Nemerow. 1993. Integrins alpha$_v$beta3 and alpha$_v$beta5 promote adenovirus internalization but not virus attachment. *Cell* 73:309–319.
14. Goldman, M. J., and J. M. Wilson. 1995. Expression of alpha v beta 5 integrin is necessary for efficient adenovirus-mediated gene transfer in the human airway. *J. Virol.* 69:5951–5958.
15. Greber, U. F., I. Singh, and A. Helenius. 1994. Mechanisms of virus uncoating. *Trends Microbiol.* 2:52–56.
16. Hong, J. S., and J. A. Engler. 1991. The amino terminus of the adenovirus fiber protein encodes the nuclear localization signal. *Virology* 185:758–767.
17. Danos, O., and R. C. Mulligan. 1988. Safe and efficient generation of recombinant retroviruses with amphotropic and ecotropic host ranges. *Proc. Natl. Acad. Sci. USA* 85:6460–6464.
18. Morgan, R. A., O. Nussbaum, D. D. Muenchau, L. Shu, L. Couture, and W. F. Anderson. 1993. Analysis of the functional and host range-determining regions of the murine ectropic and amphotropic retrovirus envelope proteins. *J. Virol.* 67:4712–4721.
19. Varmus, H. 1988. Retroviruses. *Science* 240:1427–1435.
20. Miller, D. G., M. A. Adam, and A. D. Miller. 1990. Gene transfer by retrovirus vectors occurs only in cells that are actively replicating at the time of infection. *Mol. Cell Biol.* 10:4239–4242.
21. Sahn, S. A. 1993. Pleural effusion in lung cancer. *Clin. Chest Med.* 14:189–200.
22. Mitsudomi, T., J. Viallet, J. L. Mulshine, R. I. Linnoila, J. D. Minna, and A. F. Gazdar. 1991. Mutations of ras genes distinguish a subset of non-small-cell lung cancer cell lines from small-cell lung cancer cell lines. *Oncogene* 6:1353–1362.
23. Mitsudomi, T., S. M. Steinberg, M. M. Nau, D. Carbone, D. D'Amico, S. Bodner, H. K. Oie, R. I. Linnoila, J. L. Mulshine, J. D. Minna, and A. F. Gazdar. 1992. p53 gene mutations in non-small-lung cancer cell lines and their correlation with the presence of ras mutations and clinical features. *Oncogene* 7:171–180.
24. Gazdar, A. F., R. I. Linnoila, Y. Kurita, H. K. Oie, J. L. Mulshine, J. C. Clark, and J. A. Whitsett. 1990. Peripheral airway cell differentiation in human lung cancer cell lines. *Cancer Res.* 50:5481–5487.
25. Takahashi, T., M. M. Nau, I. Chiba, M. J. Birrer, R. K. Rosenberg, M. Vinocour, M. Levitt, H. Pass, A. F. Gazdar, and J. D. Minna. 1989. p53: a frequent target for genetic abnormalities in lung cancer. *Science* 246:491–494.
26. Phelps, R. M., B. E. Johnson, D. C. Ihde, A. F. Gazdar, D. P. Carbone, P. R. McClintock, R. I. Linnoila, M. J. Matthews, P. A. Bunn, Jr., D. Carney,

J. D. Minna, and J. L. Mulshine. 1996. NCI-Navy Medical Oncology Branch cell line data base. *J. Cell Biochem. Suppl.* 24:32–91.

27. Piedimonte, G., R. J. Pickles, J. R. Lehmann, D. McCarty, D. L. Costa, and R. C. Boucher. 1997. Replication-deficient adenoviral vector for gene transfer potentiates airway neurogenic inflammation. *Am. J. Respir. Cell Mol. Biol.* 16:250–258.

28. Greber, U. F., M. Willetts, P. Webster, and A. Helenius. 1993. Stepwise dismantling of adenovirus 2 during entry into cells. *Cell* 75:477–486.

29. Adam, M. A., N. Ramesh, A. D. Miller, and W. R. A. Osborne. 1991. Internal initiation of translation in retroviral vectors carrying picornavirus 5′ nontranslated regions. *J. Virol.* 65:4985–4990.

30. Olsen, J. C., and J. Sechelski. 1995. Use of sodium butyrate to enhance production of retroviral vectors expressing CFTR cDNA. *Hum. Gene Ther.* 6:1195–1202.

31. MacGregor, G. R., and C. T. Caskey. 1989. Construction of plasmids that express *E. coli* beta-galactosidase in mammalian cells. *Nucleic Acids Res.* 17:2365.

32. Batra, R. K., H. Berschneider, and D. T. Curiel. 1994. Molecular conjugate vectors mediate efficient gene transfer into gastrointestinal epithelial cells. *Cancer Gene Ther.* 1:185–192.

33. Batra, R. K., J. C. Olsen, D. K. Hoganson, B. Caterson, and R. C. Boucher. 1997. Retroviral gene transfer is inhibited by chondroitin sulfate proteoglycans/glycosaminoglycans in malignant pleural effusions. *J. Biol. Chem.* 272:11736–11743.

34. Krasnykh, V. N., G. V. Mikheeva, J. T. Douglas, and D. T. Curiel. 1996. Generation of recombinant adenovirus vectors with modified fibers for altering viral tropism. *J. Virol.* 70:6839–6846.

35. Yankaskas, J. R., J. E. Haizlip, M. Conrad, D. Koval, E. Lazarowski, A. M. Paradiso, R. Schlegel, B. Sarkadi, and R. C. Boucher. 1993. Papilloma virus immortalized tracheal epithelial cells retain a well-differentiated phenotype. *Am. J. Physiol.* 264:C1219–C1230.

36. Finney, D. J. 1971. Probit Analysis. Cambridge University Press, London.

37. Hart, P. J., J. C. Olsen, L. G. Johnson, R. J. Pickles, S. Randell, and R. C. Boucher. 1996. Reduced retroviral entry into polarized airway epithelia. *Pediatr. Pulmonol. Suppl.* 13:278. (Abstr.)